MODELING OF AN ABSORPTION REFRIGERATOR DRIVEN BY THE DIRECT COMBUSTION OF NATURAL GAS

Yipsy Roque Benito, gipsyrb@mec.puc-rio.br
José Alberto Reis Parise, parise@mec.puc-rio.br
Pontifícia Universidade Católica de Rio de Janeiro, Departamento de Engenharia Mecânica. Rua Marquês de São Vicente, 225, Gávea. 22453-900 Rio de Janeiro, RJ, Brazil

José Viriato Coelho Vargas, jvargas@demec.ufpr.br
Universidade Federal do Paraná, Departamento de Engenharia Mecânica, Caixa Postal 19011, 81531-990 Curitiba, PR, Brazil

Abstract. *The present study is part of a more comprehensive project whose objective is the study of absorption refrigeration systems from waste heat (DORAGEX). A mathematical model, describing the thermodynamic behavior of an existing absorption refrigerato, driven by the direct combustion of natural gas, was developed. The single-effect water-ammonia refrigeration cycle is characterized by a number of internal regeneration features which improve its efficiency yet posing further complexities in its simulation. The resulting set of algebraic non-linear equations was solved with software EES. In view of the absence of detailed information on equipment characteristics, a semi-empirical approach was adopted, based on experimental data from an existing apparatus.*

Keywords*: absorption refrigeration, simulation, modeling, natural gas*

1. INTRODUCTION

The water-ammonia absorption cycle has long been applied for refrigeration purposes. Ammonia is the refrigerant and water, the absorbent. This cycle can be applied whenever ammonia use as refrigerant is adequate. Fundamentals of absorption refrigeration can be found in textbooks and handbooks (e.g., Perry et al., 1975; Faires, 1978; Perry, 1997). Likewise, modeling and simulation of such systems have been extensively dealt with. Simulation models can be classified as fundamental, empirical and semi-empirical. Solution is, generally, numerical (e.g., Grossman, 1983, 2001; Grossman and Heath, 1984), with graphical solutions being found in earlier works (Threlkeld, 1970). Extensive work on absorption cycle simulation can be found in the literature. For example, Patnaik and Perez-Blanco (1993), Ng et al. (2000) and Fernández-Seara et al. (2002) present recent analyses on the heat and mass transfer processes that take place during distillation in absorption cycles. Several cycle configurations have been modeled, like open and semi-open cycles and single cycles (Morejón and Brum, 2001). This work presents a semi-empirical modeling effort of a single stage multi-regeneration water-ammonia absorption refrigeration cycle, based on fundamental conservation equations. Experimental data, to support the model with characteristics of cycle components, were taken from Pereira (2006) who tested a gas-fired water(or ethylene glycol water solution)-to-water absorption ROBUR 5 TR heat pump, model GAHP-W (Robur, 2005). Pereira (2006) obtained, for different operation conditions, water temperatures and mass flow rates from condenser and evaporator as well as fuel consumption.

2. SYSTEM DESCRIPTION

Figure 1 shows the thermodynamic cycle to be modeled, with components and thermodynamic states. Pressure and temperature levels are qualitatively depicted. Work and heat transfer rates are also indicated. Ammonia vapor (14) flows from the evaporator to the pre-absorber, where it mixes with the weak solution (6), which is a result of the desorption process in the generator. The resulting mixture is a strong solution (15), which flows through the water-cooled absorber, where rejects heat to the warm water circuit, thus completing the absorption process. The pump raises the pressure of the strong solution (2) to that of the generator. It is then heated up to (16), in the rectifier, and to (3), in the pre-absorber. In the generator, desorption takes place, with ammonia vapor (7) being separated from the strong solution, weakening it (4). An expansion device reduces the pressure of the weak solution (6) before it enters the absorber to reinitiate the cycle. Vapor (7), on the other hand, enters the rectifier, where the ammonia concentration is augmented through condensation. The liquid reflux (8) returns to the generator and ammonia vapor (9) enters the condenser. The sequence of condenser (9-10), expansion devices (10-17) and (11-12), regenerator, or refrigerant heat exchanger, (17-11), and evaporator (12-13), is similar to that of a vapor-compression heat pump. This particular absorption cycle (Robur, 2005) is characterized by the pre-heating of the strong solution in the rectifier and in the absorber and by pre-heating of ammonia vapor before entering the absorber. All these three operations take place dispensing with the existence of an external heat source, which poses some intrinsic complications for both the design and simulation of such cycle.

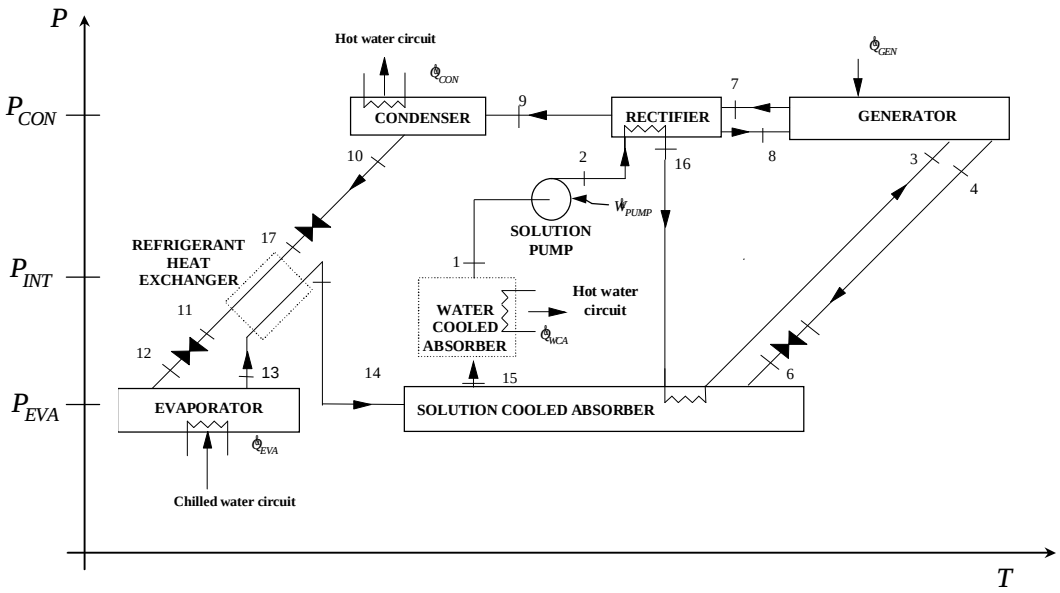

Figure 1. Schematic diagram and pressure and temperature levels of the absorption heat pump cycle with internal regeneration.

3. MATHEMATICAL MODEL

The model is based on the application of fundamental mass and energy conservation equations to each component of the cycle (lumped parameter analysis). Equations for the heat and mass transfer processes and for refrigerant and absorbent thermodynamic properties are also applied. The model employs the heat and mass transfer effectiveness concept for the exchangers. It is believed that this approach simplifies the exchangers modeling, for effectiveness values lie between zero and unity, useful range for a situation where very little information on component characteristics is available.

3.1 Simplifying assumptions

The following assumptions were adopted: i) The cycle operates at steady-state; ii) Water (absorbent) does not vaporize in the generator, so that on pure refrigerant (ammonia) circulates between the evaporator and the condenser; iii) Pressure drop across tubing and components is not considered; iv) Component irreversibility is accounted for through its efficiency; v) Properties of the ammonia-water mixture are determined from library NH3H2O of EES program (EES, 2004). This thermodynamic property subroutine is based on equations presented by Ibrahim and Klein (1993). More assumptions will follow as the mathematical model is presented.

3.2 Pressure levels determination

From hypothesis (iii), it can be concluded that the cycle operates within three pressure levels, P_{CON} , P_{INT} and P_{EVA} established by the pump and expansion devices. The intermediate pressure is set to provide an adequate temperature level for the internal regeneration process (17-11). Condensing and evaporating pressures are mostly influenced, respectively, by heat sink and heat source temperatures, as follows.

3.2.1 Condensing pressure

The condensing temperature, T_{CON} , was assumed to be above the cooling water inlet temperature, $T_{hw_{in}}$, by a difference of ΔT_{CON} .

$$T_{CON} = T_{hw_{in}} + \Delta T_{CON} \tag{1}$$

$$P_{CON} = P_{sat}\left(T_{CON}\right) \tag{2}$$

This difference, ΔT_{CON}, is dependent on the condenser water mass flow rate, $\dot{m}_{hw}$. From experimental evidence (Parise, 1983), condensing pressure, P_{CON}, is maximum when the water flow rate is minimum, and vice-versa. A linear variation was adopted for ΔT_{CON}. Values for the limits of both water mass flow rate and temperature ranges, $\dot{m}_{hw;\max}$, $\dot{m}_{hw;\min}$, $\Delta T_{CON;\max}$ and $\Delta T_{CON;\min}$ were taken from tests on an existing apparatus (Pereira, 2006).

$$\Delta T_{CON} = \Delta T_{CON;\min} + \left(\frac{\dot{m}_{hw;\max} - \dot{m}_{hw}}{\dot{m}_{hw;\max} - \dot{m}_{hw;\min}} \right) \left(\Delta T_{CON;\max} - \Delta T_{CON;\min} \right) \tag{3}$$

3.2.2 Evaporating pressure

An analogous rationale was applied for the determination of the evaporating pressure, P_{EVA}. This time, the evaporating temperature is, of course, below the water (or solution) inlet temperature, $T_{cw_{in}}$, and the temperature difference, ΔT_{EVA}, increases with the mass flow rate, $\dot{m}_{cw}$.

$$T_{EVA} = T_{cw_{in}} - \Delta T_{EVA} \tag{4}$$

$$P_{EVA} = P_{sat}\left(T_{EVA}\right) \tag{5}$$

$$\Delta T_{EVA} = \Delta T_{EVA;\max} + \left(\frac{\dot{m}_{cw;\max} - \dot{m}_{cw}}{\dot{m}_{cw;\max} - \dot{m}_{cw;\min}} \right) \left(\Delta T_{EVA;\max} - \Delta T_{EVA;\min} \right) \tag{6}$$

3.2.3 Intermediate pressure

The intermediate pressure derives from the balance between the two ammonia expansion devices, (10-17 and 11-12), which are short tube orifices (Robur, 2005). For their modeling, the following assumptions were adopted: (vi) Refrigerant is at saturated condition (liquid) at the entrance of both orifices; (vii) The intermediate to condensing pressure ratio is constant throughout the operation of the heat pump. Hypothesis (vii) is based on the study on modeling of flow through short tube orifices, carried out by Aaron and Domanski (1989, 1990), who showed a strong dependence of the mass flow rate with geometry (length, orifice diameter and chamfer angle) and upstream conditions (pressure and degree of subcooling). A semi-empirical model was presented, providing the mass flow rate in terms of a reference mass flow rate multiplied by three correction factors, Φ_1, Φ_2 and Φ_3 (ASHRAE, 2006). Two of these factors are dependent on the geometry of the orifice, which, of course, does not change for a given heat pump. The other, is dependent on the degree of subcooling, upstream the orifice, also invariant for given equipment, following assumption (vi). Besides, from the results of Aaron and Domanski (1989, 1990), a simple relation between the reference mass flow rate, $\dot{m}_{ref}$, and the pressure upstream the orifice, $P_{upstream}$, can be established, as follows:

$$\dot{m}_{ref} = a\, P_{upstream}^{S} \tag{7}$$

where coefficient a and exponent S are dependent on the degree of subcooling. From assumption (vi):

$$\dot{m}_{ref,high} = a\, P_{CON}^{S} \tag{8}$$

$$\dot{m}_{ref,low} = a\, P_{INT}^{S} \tag{9}$$

The mass flow rate across each orifice is the same, Fig. 1, so that:

$$\dot{m} = \dot{m}_{ref,high}\Phi_{1,high}\Phi_{2,high}\Phi_{3,high} = \dot{m}_{ref,low}\Phi_{1,low}\Phi_{2,low}\Phi_{3,low} \tag{10}$$

From equations (7) to (10), one can define a factor, Φ, which does not vary with the heat pump operational conditions:

$$\frac{\dot{m}_{ref,high}}{\dot{m}_{ref,low}} = \frac{\Phi_{1,low}\Phi_{2,low}\Phi_{3,low}}{\Phi_{1,high}\Phi_{2,high}\Phi_{3,high}} = \frac{P_{CON}^{S}}{P_{INT}^{S}} = \Phi^{-S} \tag{11}$$

Equation (11) provides a simple relation between the condensing and intermediate pressures, which is valid for all operational conditions, provided that the established assumptions are met. Parameter Φ becomes a pressure ratio factor.

$$P_{INT} = \Phi P_{CON} \tag{12}$$

3.3 Mass and energy balances

3.3.1 Ammonia cycle

The circuit comprising states 9 to 14, in Fig. 1, constitutes the ammonia cycle, so called because the ammonia concentration in this part of the cycle is very close to unity (Benito, 2007). In fact, from assumption (ii), pure ammonia is considered in the present analysis. The P-h diagram of the ammonia cycle, comprising the condenser, expansion devices, refrigerant heat exchanger and evaporator, is presented in Fig. 2. Refrigerant vapor, from the rectifier, condenses (9-10), rejecting heat to the heat sink (warm water circuit), and expanding (10-17), in the high pressure orifice, to the intermediate pressure. In the internal refrigerant-to-refrigerant heat exchanger, the two-phase stream rejects heat (17-11) to the vapor stream that leaves the evaporator, increasing its enthalpy (13-14), before entering the absorber. Leaving the heat exchanger as saturated liquid, assumption (vi), refrigerant further expands in the low pressure orifice (11-12), before entering the evaporator at evaporating pressure. Heat is then removed (12-13) from the heat source (chilled water or ethylene-glycol solution stream), reducing its temperature. Lack of space precludes the presentation of the full treatment given to the modeling of the ammonia cycle, which can be found in Benito (2007).

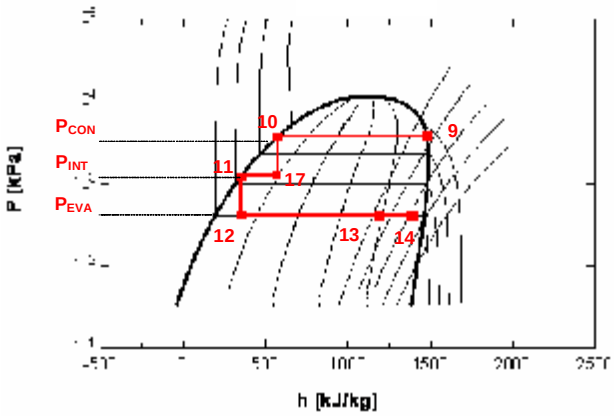

Figure 2. P - h diagram of the ammonia cycle

3.3.2 Thermal compressor

In the absorption refrigeration cycle, high pressure pure ammonia vapor (9) is the result of a series of processes that comprise the so called “thermal compressor”. It is composed of, Fig. 1, the strong solution-cooled absorber (SCA), the water-cooled absorber (WCA), the solution pump (PUMP), rectifier (REC), generator (GEN) and expansion device (6-4). These processes are deeply interconnected. Ammonia vapor from the evaporator (14) enters the absorber, mixes with the weak solution from the generator (6), to form a strong solution (15), which is then cooled (15-1), pumped (1-2) and pre-heated (2-16), to enter the generator, after it circulates through the absorber coil (16-3). The generator produces the high pressure vapor, with a high content of ammonia which, after rectification (7-8-9/2-16), flows to the condenser, for heat rejection. The mathematical modeling of the thermal compressor is detailed in the sections that follow.

3.3.2.1 Absorption process

The absorption process takes place into two stages: cooled by the strong solution (SCA) and by water (WCA).

3.3.2.1.1 Pre-absorber or absorber-regenerator

In the pre-absorber, Fig. 3a, ammonia vapor from the evaporator (14) is mixed to the weak solution (6) and cooled by the strong solution (16-3) that circulates in the coil, downstream its pre-heating from rectification heat (2-16). These processes are drawn in the enthalpy-concentration diagram, in Fig. 3b.

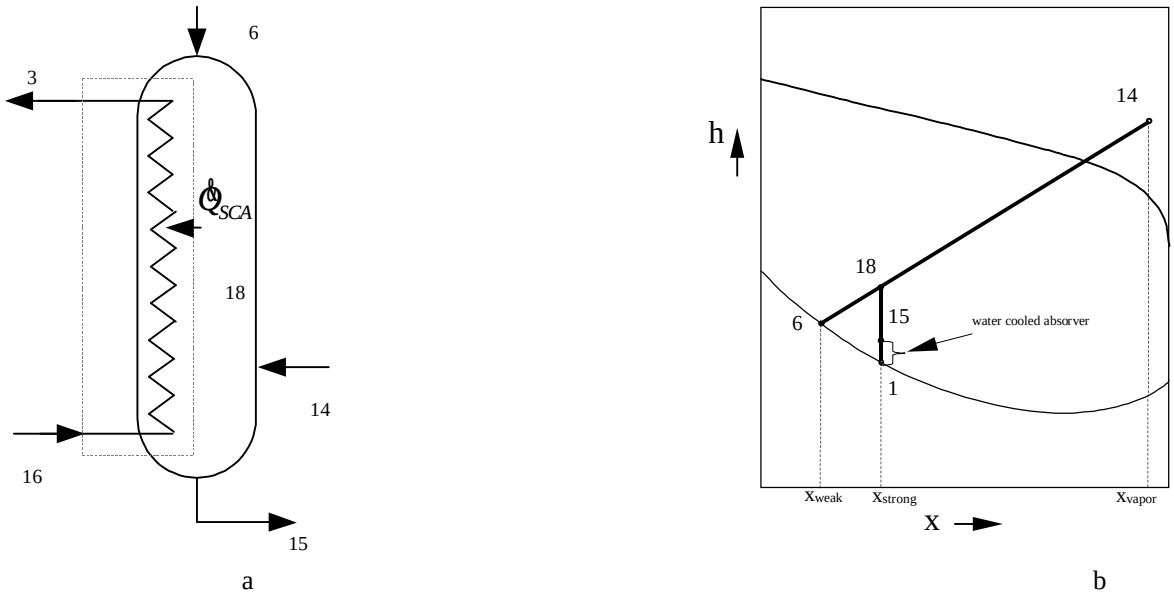

Figure 3. Pre-absorber: (a) Control volume; (b) Enthalpy-concentration diagram, $h-x$.

The following hypotheses are assumed: (viii) Vapor (14) and liquid (6) entering the pre-absorber inlet are at the same pressure, P_{EVA}, but not at thermal equilibrium; (ix) The process (SCA) takes place at constant pressure, P_{EVA}; (x) The process is divided into two independent and sequential processes, namely, an adiabatic mixture between the two streams (6-14-18), followed by cooling (18-15). Overall and ammonia mass balances provide:

$$\dot{m}_6 + \dot{m}_{14} = \dot{m}_{15} \tag{13}$$

$$\dot{m}_6 x_6 + \dot{m}_{14} x_{14} = \dot{m}_{15} x_{15} \tag{14}$$

The energy conservation equations, in the shell and coil sides, provide the pre-absorber heat transfer rate, $\dot{Q}_{SCA}$:

$$\dot{Q}_{SCA} = \dot{m}_{15} h_{15} - \dot{m}_6 h_6 - \dot{m}_{14} h_{14} \tag{15}$$

$$\dot{Q}_{SCA} = \dot{m}_3 h_3 - \dot{m}_{16} h_{16} \tag{16}$$

From assumption (x), the global and ammonia mass and energy balances, for the adiabatic mixing, provide, respectively:

$$\dot{m}_6 + \dot{m}_{14} = \dot{m}_{18} \tag{17}$$

$$\dot{m}_6 x_6 + \dot{m}_{14} x_{14} = \dot{m}_{18} x_{18} \tag{18}$$

$$\dot{m}_6 h_6 + \dot{m}_{14} h_{14} = \dot{m}_{18} h_{18} \tag{19}$$

The absorber is, essentially, a heat and mass transfer equipment. To evaluate the heat transfer rate, $\dot{Q}_{SCA}$, the concept of heat and mass transfer effectiveness, $e_{h;SCA}$, as studied by Islam and Wijeysundera (2006) and Patnaik and Perez-Blanco (1993), is here applied. Maximum mass absorption rate would occur in an ideal absorber where the solution would be cooled to the inlet temperature of the cooling fluid (the strong solution flowing inside the coil), T_{16}. The solution would reach the equilibrium concentration corresponding to T_{16}. Maximum heat transfer would also take place under such conditions (Patnaik and Perez-Blanco, 1993). Therefore, the pre-absorber effectiveness can be defined as in equation(20), below.

$$e_{h;SCA} = \frac{\dot{Q}_{SCA}}{\dot{Q}_{SCA,\max}} = \frac{h_{18} - h_{15}}{h_{18} - h_{15(T_{15}=T_{16})}} \tag{20}$$

3.3.2.1.2 Water-cooled absorber

The following assumptions apply for the modeling of this equipment: (xi) The capacity rate of the solution is always greater that of the cooling water, $\dot{m}_{hw} c_{p_w}$; (xii) The strong solution leaves the water-cooled absorber (1) as saturated liquid. Mass and energy balances, the latter for the solution and water sides, are, respectively:

$$\dot{m}_{15} = \dot{m}_1 \tag{21}$$

$$\dot{Q}_{WCA} = \dot{m}_1 \left(h_{15} - h_1 \right) \tag{22}$$

$$\dot{Q}_{WCA} = \dot{m}_{hw} c_{p_w} \left(T_{hw;out} - T_{hw;out;CON} \right) - \dot{Q}_{n;WCA} \tag{23}$$

Noting that, in this specific heat pump, the absorber cooling water comes from the condenser, so that the inlet temperature is $T_{hw;out;CON}$, the heat transfer effectiveness is defined as follows:

$$e_{h;WCA} = \frac{\dot{Q}_{WCA}}{\dot{Q}_{WCA;\max}} = \frac{\dot{Q}_{WCA}}{\dot{m}_{hw} c_{pw} \left(T_{15} - T_{hw;out;CON} \right)} \tag{24}$$

Thermal losses, $\dot{Q}_{n;WCA}$, from the solution (shell side) to ambient, have been computed for this heat exchanger. They are accounted for, by means of a loss coefficient, q_{WCA}, as a percentage of the thermal power that goes to the water coil.

$$\dot{Q}_{n;WCA} = q_{WCA} \dot{Q}_{WCA} \tag{25}$$

3.3.2.2 Solution pump

The pump has two purposes: to circulate of the working fluid and to establish a pressure difference across the system. Overall and ammonia mass balances are:

$$\dot{m}_1 = \dot{m}_2 \tag{26}$$

$$x_1 = x_2 \tag{27}$$

The pumping power, $\dot{W}_{PUMP}$, is determined based on constant liquid specific volume, v_2, and on a given isentropic efficiency, h_{PUMP}, defined below. State $2s$ corresponds to an ideal isentropic pumping process.

$$\dot{W}_{PUMP} = 100\left(P_2 - P_1\right)\frac{v_2 \dot{m}_2}{h_{PUMP}} \tag{28}$$

$$h_{PUMP} = \frac{h_{2S} - h_1}{h_2 - h_1} \tag{29}$$

3.3.2.3 Rectifier

Ammonia purification, Fig. 4a, takes place at the rectifier due to internal heat removal, $\dot{Q}_{REC}$. The following assumptions are applied: (xiii) Vapor enters the rectifier as dry saturated; (xiv) Vapor (9) and reflux (16) leave the rectifier at thermal equilibrium; (xv) Process (7-8-9) takes place at constant pressure, P_{CON}; (xvi) The heat transfer process (7-20) is supposed to occur before adiabatic liquid separation (20-9-8), Fig. 4b.

Figure 4 Rectification: (a) Control volume; (b) "Preliminary" heat removal process.

Shell (overall and ammonia) and coil sides mass balances are:

$$\dot{m}_7 = \dot{m}_9 + \dot{m}_8 \tag{30}$$

$$\dot{m}_{16} = \dot{m}_2 \tag{31}$$

$$\dot{m}_7 x_7 = \dot{m}_9 x_9 + \dot{m}_8 x_8 \tag{32}$$

Equations (33) to (36) describe the mass and energy balances for the heat transfer process; bearing in mind that state (20) corresponds to a hypothetical thermodynamic state, assumption (xvi). Note that states (8) and (9) represent the saturated liquid and vapor phases, respectively, of state (20). Vapor quality is represented by q.

$$\dot{m}_{20} = \dot{m}_7 \tag{33}$$

$$\dot{m}_8 = \dot{m}_{20}\left(1 - q_{20}\right) \tag{34}$$

$$\dot{m}_9 = \dot{m}_{20} q_{20} \tag{35}$$

$$\dot{Q}_{REC} = \dot{m}_7\left(h_7 - h_{20}\right) \tag{36}$$

Equations (37) and (38) provide the coil side energy balance and the definition of the rectifier effectiveness, $e_{h;REC}$.

$$\dot{Q}_{REC} = \dot{m}_2\left(h_{16} - h_2\right) \tag{37}$$

$$e_{h;REC} = \frac{\dot{Q}_{REC}}{\dot{Q}_{REC;\max}} = \frac{\dot{Q}_{REC}}{\dot{m}_2 c_{p_2} \left(T_7 - T_2\right)} \tag{38}$$

3.3.2.4 Generator

In the case studied, heat pump Robur model GAHP-W (Pereira, 2006), the generator was a distillation column. Gas combustion provides the heat to gradually vaporize the solution. Vapor exchanges heat and mass, first, with the liquid that feeds the column and, then, with the reflux from the rectifier. The ascending vapor has its temperature gradually reduced. For the modeling of the generator, a single control volume, Fig.5, was employed. It is assumed that: (xvii) The process takes place at constant pressure throughout.

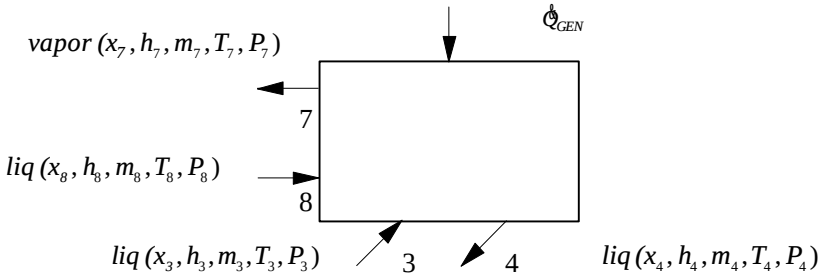

Figure 5. Generator control volume

Mass (overall and ammonia) and energy balance equations are:

$$\dot{m}_3 + \dot{m}_8 = \dot{m}_4 + \dot{m}_7 \tag{39}$$

$$\dot{m}_3 x_3 + \dot{m}_8 x_8 = \dot{m}_4 x_4 + \dot{m}_7 x_7 \tag{40}$$

$$\dot{Q}_{GEN} + \dot{m}_3 h_3 + \dot{m}_8 h_8 = \dot{m}_7 h_7 + \dot{m}_4 h_4 \tag{41}$$

3.3.2.5 Expansion device of the thermal compressor

Like the ammonia cycle, the thermal compressor operates between two pressure levels, requiring an expansion device, also a short tube orifice, to regulate the flow between the generator and the absorber. The mass and energy balances are:

$$\dot{m}_6 = \dot{m}_4 \tag{42}$$

$$x_6 = x_4 \tag{43}$$

$$h_6 = h_4 \tag{44}$$

4 Solution

The mathematical model depicted above was solved with software EES (EES, 2004). This software uses the Newton-Rhapson method to solve systems of non-linear algebraic equations.

4.1 Simulation

The model was employed to simulate the absorption chiller from Robur, model GAHP-W, as tested by Pereira (2006). Only external experimental data were available at the time of the simulation, being restricted to inlet and outlet

temperatures and mass flow rates of water streams and gas consumption rate. In view of this limitation, the model development took, from the start, a semi-empirical approach, with system components being characterized by overall empirical parameters, as seen on the equations above. Still, fundamental conservation equations were kept for all components. The model was set to simulate all experimental runs from Pereira (2006) and the empirical parameters were adjusted to best fit experimental results. The following parameters were determined by this approach and were kept constant throughout the simulation effort: ammonia concentration in the ammonia cycle, $x_9 = 1$; condenser effectiveness, $e_{h;CON} = 0.5$; condenser loss coefficient, $q_{CON} = 0.2$; evaporator effectiveness, $e_{h;EVA} = 0.3$; evaporator heat gain coefficient, $q_{EVA;\max} = 0.1$; saturated liquid at the internal regenerator outlet, $q_{11} = 0$; short tube orifice pressure ratio, $\Phi = 0.8$; strong solution cooled heat exchanger effectiveness, $e_{h;SCA} = 0.9$; absorber coolant inlet temperature, $T_{16} = 351K$; strong solution vapor quality at absorber inlet, $q_1 = 0$; loss coefficient of water cooled absorber, $q_{WCA} = 0.2$; pump efficiency, $h_{PUMP} = 0.9$; rectifier effectiveness, $e_{h;REC} = 0.3$. Finally, the mass flow rate of the weak solution was considered to be 85% to that of the strong solution.

5. COMPARISON WITH EXPERIMENTAL DATA

The program was fed with experimental data from Pereira (2006), namely, the external fluid mass flow rates and inlet temperatures, and predicted the outlet temperatures and thermal power rates. Figs. 6a and 6b present the comparison between exit temperatures of the water-ethylene glycol mixture and condenser water flows and their corresponding experimental values. Fig. 7 shows the comparison for the evaporator and rejected heat rates. Overall, it can be said that reasonable agreement was obtained.

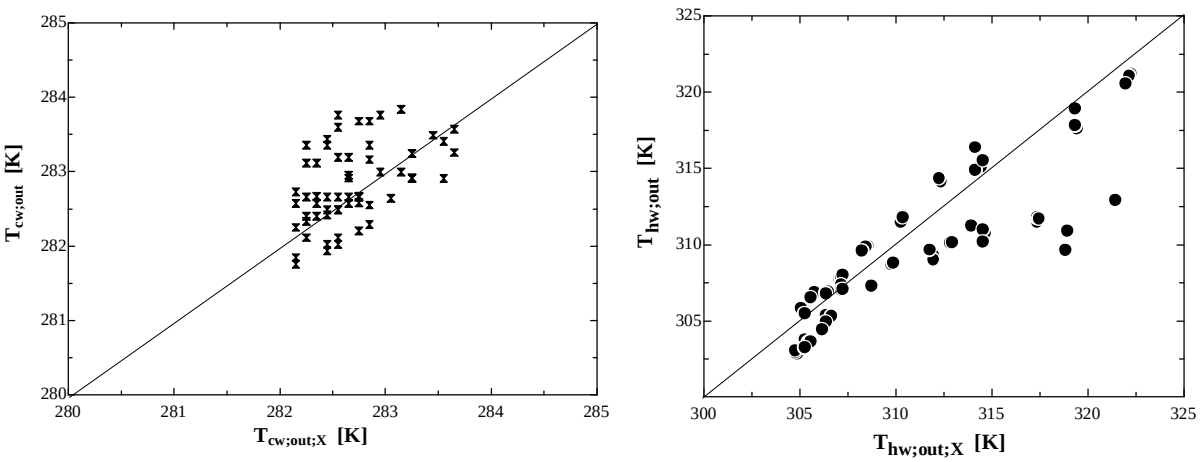

Figure 6. Comparison between predicted and experimental values. (a) Chilled water-etylene glycol solution; (b) condenser water

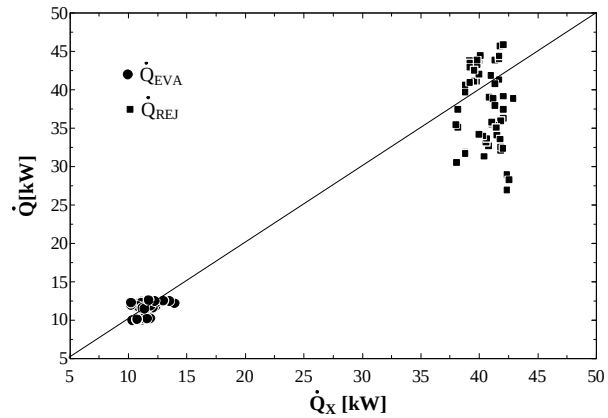

Figure 7. Comparison between predicted and experimental values of the thermal power rates (evaporator and rejection)

5. CLOSURE

A semi-empirical model, based on a limited number of known experimental variables, yet employing fundamental conservation equations, was developed and tested. In spite of its inherent limitations, the model showed reasonable agreement with experimental data verification. Not shown in the present work, the model was able to perform optimization tests of the heat pump (Benito, 2007), with predicted optimal results close to those measured by Pereira (2006).

6. ACKNOWLEDGEMENTS

The authors gratefully acknowledge the financial support from ANP, CNPq, FAPERJ, FINEP and Grupo Nilko.

7. REFERENCES

Aaron, D.A. and P.A. Domanski. 1990. Experimentation, analysis, and correlation of Refrigerant-22 flow through short tube restrictors. ASHRAE Transactions 96(1):729-742.

Aaron, D.A., Domanski, P.A., An experimental investigation and modeling of the flow rate of refrigerant 22 through the short tube restrictor, NISTIR 89-4120, National Institute of Standards and Technology, July 1989.

ASHRAE, ASHRAE Handbook, Refrigeration – Systems and Applications, Chapter 44: Refrigerant-Control Devices, 2006, SI edition.

Benito, Y. R., Modelagem da produção simultânea de frio, calor e energia elétrica. Dissertação de Mestrado. Departamento de Engenharia Mecânica, Pontificia Universidade Católica de Rio de Janeiro, 2007

Chua, H. T., Toh, H. K.,. Malek, A., K.C. Ng, K., Srinivasan, N, A general thermodynamic framework for understanding the behavior of absorption chillers. International Journal of Refrigeration 23 (2000) 491±507

Engineering Equation Solver (EES), version V7,258-3D, F-Chart Software, LLC.

Faires, V., M.; Simmang, C. M. Thermodynamics /. 6. ed. - New York : Macmillan, c1978. 647p.

Fernãndez-Seara, J., Sieres, J. Amônia-water absorption refrigeration system with flooded evaporators, Applied Thermal Engineering 26 (2006) 2236-2246

Fernández-Seara, J. Sieres, J., M. Vázquez, Simultaneous heat and mass transfer of a packed distillation column for ammonia–water absorption refrigeration systems, International Journal Thermal Science, 41 (2002) 927–935.

Grossman, ABSIM: modular simulation of advanced absorption systems, International journal of refrigeration 24 (2001) 531-543.

Grossman, G., Heath, M. T., Simultaneous heat and mass transfer in absorption of gases in turbulent liquids, Int. J. Heat MassTransfer 27 (12) (1984) 2365–2376.

Grossman, G., Simultaneous heat and mass transfer in film absorption under laminar flow, Int. J. Heat Mass Transfer 6 (3) (1983) 357– 371.

Ibrahim, O.M. and Klein S.A., “Thermodynamic Properties of Ammonia-Water Mixtures”, ASHRAE Transactions, CH-93-21-2 January, 1993. 99(1), 1495-1502.

Islam, R. Wijeysundera, N.E., Ho, J. C., Heat and mass transfer effectiveness and correlations for counter-flow absorbers Int. J. Heat Mass Transfer 49 (2006) 4171-4182.

Morejón, C. F. M., Brum, N.C. L., Exergetical análisis for optimization of the componets of the absorption refrigeration cycles whith water-ammonia asworking fluid., Proceedings of COBEM 2001, Refrigeration, Air conditioning,Heating and Ventilation. Vol 5, 2001.

Ng, K. C., Chua, H. T., and Han, Q., On the modeling of absorption chillers with external and internal irreversibilities Applied Thermal Engineering Vol. 17, No. 5, 1997, pp. 413-425,

Parise,J.A.R.,Theoretical and experimental analysis of a diesel engine driven heat pump, UMIST, Manchester, Inglaterra,1983

Patnaik, V., Perez-Blanco H., A counter flow heat-exchanger analysis for the design of falling film absorbers, Int. Absorption Heat Pump Conf. AES-31 (1993) 209–216]

Pereira, M. A., Análise exergética experimental de uma unidade de refrigeração por absorção de 5TR movida a gás liquefeito de petróleo (GLP). Dissertação de Mestrado. Setor de Tecnologia, Universidade Federal de Paraná, 2006.

Perry, R. H.; Green, D. W.; Maloney, J. O. Perry's chemical engineers' handbook. 7th ed. Mew York: McGraw-Hill, 1997. 1 v.

Robur, S. A. Installation, start up and maintenance manual. Bergamo, Italia. 2005

Threlkeld, J. L., Thermal environmental engineering. 2. ed. Englewood Cliffs, N.J.: Prentice-Hall, 1970. 495 p.

7. RESPONSIBILITY NOTICE

The authors are the only responsible for the printed material included in this paper.